Birck Nanotechnology Center

Birck and NCN Publications

Purdue Libraries *Year* 2006

Fabrication and characterization of solid-state nanopores using a field emission scanning electron microscope

Hung Chang* Samir Iqbal† E A. Stach‡
Alexander H. King** Nestor J. Zaluzec†† Rashid Bashir‡‡

*Birck Nanotechnology Center and School of Electrical and Computer Engineering, Purdue University,, hc@purdue.edu

†Birck Nanotechnology Center and School of Electrical and Computer Engineering, Purdue University, smiqbal@purdue.edu

‡Birck Nanotechnology Center and School of Materials Engineering, Purdue University, eastach@purdue.edu

**Birck Nanotechnology Center and School of Materials Engineering, Purdue University, alexking@purdue.edu

††Electron Microscopy, Materials Sciences, Division, Argonne National Laboratory

‡‡Birck Nanotechnology Center, School of Electrical and Computer Engineering, Weldon School of Biomedical Engineering, School of Mechanical Engineering, Purdue University, bashir@purdue.edu

This paper is posted at Purdue e-Pubs.

http://docs.lib.purdue.edu/nanopub/4

Fabrication and characterization of solid-state nanopores using a field emission scanning electron microscope

Hung Chang and Samir M. Iqbal
Birck Nanotechnology Center and School of Electrical and Computer Engineering, Purdue University, West Lafayette, Indiana 47907

Eric A. Stach and Alexander H. King
Birck Nanotechnology Center and School of Materials Engineering, Purdue University, West Lafayette, Indiana 47907

Nestor J. Zaluzec
Electron Microscopy Center, Materials Sciences Division, Argonne National Laboratory, Argonne, Illinois 60439

Rashid Bashir[a]
Birck Nanotechnology Center, School of Electrical and Computer Engineering, Weldon School of Biomedical Engineering, School of Mechanical Engineering, Purdue University, West Lafayette, Indiana 47907

(Received 20 June 2005; accepted 31 January 2006; published online 8 March 2006)

The fabrication of solid-state nanopores using the electron beam of a transmission electron microscope (TEM) has been reported in the past. Here, we report a similar method to fabricate solid-state nanopores using the electron source of a conventional field-emission scanning electron microscope (FESEM) instead. Micromachining was used to create initial pore diameters between 50 nm and 200 nm, and controlled pore shrinking to sub 10 nm diameters was performed subsequently during *in situ* processing in the FESEM. Noticeably, different shrinking behavior was observed when using irradiation from the electron source of the FESEM than the TEM. Unlike previous reports of TEM mediated pore shrinkage, the mechanism of pore shrinkage when using the FESEM could be a result of surface defects generated by radiolysis and subsequent motion of silicon atoms to the pore periphery. © *2006 American Institute of Physics*. [DOI: 10.1063/1.2179131]

The use of single ion channels to probe biological molecules has attracted the attention of researchers from various areas since Kasianowicz *et al.* reported ionic current measurements of DNA translocation through an α-hemolysin nanopore.[1] The basic idea of such measurements is that a single nanopore in a membrane provides the only path for DNA transport between *cis* and *trans* chambers under electrophoresis. When DNA traverses the pore, fluctuations in the ionic currents are observed. Following Kasianowicz's work, researchers have used micromachining techniques to fabricate solid-state nanopores, in an attempt to replicate the biological analogs, as the solid-state ones are more robust and stable in various chemical environments.[2,3] These solid-state nanopore analogs have been successfully utilized to perform measurements identical to the biological ion channels.[4,5] Electron beam-induced shrinkage of pores using a transmission electron microscope source, and subsequent DNA electrophoresis measurements with those pores have been recently reported.[3–6] Using a surface tension argument, Storm *et al.*[3] proposed that if the diameter of a pore is greater than the thickness of the oxide coating, the pore will expand while being exposed to the electron beam in the TEM; otherwise, the pore will shrink. In this paper, we report that pore shrinkage can be obtained using the electron source from a field emission scanning electron microscope as well. In contrast to the prior TEM work, pore shrinkage is found to be independent of the initial pore dimension and pore expansion is never observed. This new technique allows precise control on the pore diameter through use of *in situ* observation, thereby providing wider latitude on the selection of initial pore size.

The samples were prepared using similar processes reported in the literature, up to the point of shrinking the pore diameter.[3,5,6] SIMOX silicon on insulator (SOI) wafers doped with boron to a concentration of 1×10^{19} No./cm^3 were used as the initial substrates for microfabrication. Utilizing e-beam lithography, 80–100 nm dots were written on the front side of the wafer. The e-beam resist was 250 nm thick ZEP 7000, and the dose was 135 μC/cm^2. Reactive ion etching was used to open holes in the oxide through the dots, and was followed by an anisotropic wet etch from the back side of the wafer to create a thin membrane. A 100–150 nm wide pore was opened in the membrane after the SOI membrane was anisotropically wet etched from the front side and the buried oxide layer (BOX) was removed. Finally, 100 nm of thermal oxide was grown. This oxidation reduced the pore size to around 50–100 nm and resulted in ~30 nm thick SOI layer. This structure is shown in Fig. 1(a). Three additional structures, shown in Figs. 1(b)–1(d), were also fabricated and used to explore pore shrinkage. Sample B was a pore contained in a silicon membrane without any oxide. Sample C had the pore in the SOI layer but the BOX layer was not removed. This resulted in a 120 nm pore in the overhang oxide layer. Sample D had a pore in the SOI layer without the overhang oxide, and the BOX layer was not removed. All of the samples were processed and observed in Field-emission scanning electron microscope (FESEM) after preparation.

Our pore resizing experiments were conducted in a Hitachi S-4800 FESEM operating at accelerating voltages

[a]Electronic mail: bashir@purdue.edu

 © 2006 American Institute of Physics
Downloaded 27 Mar 2006 to 128.211.249.94. Redistribution subject to AIP license or copyright, see http://apl.aip.org/apl/copyright.jsp

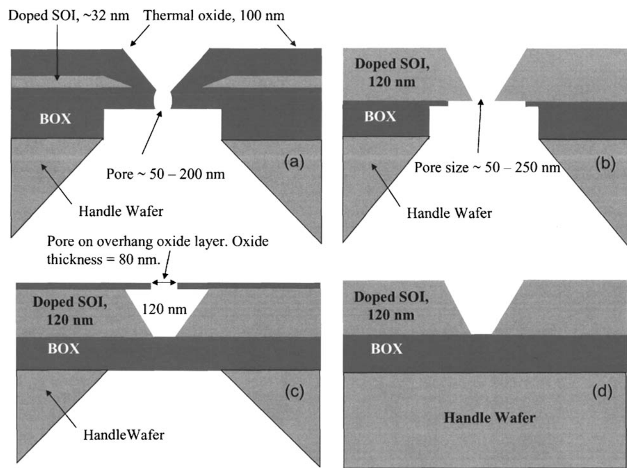

FIG. 1. Cross sections of the samples presented in this paper. (a) Sample A; (b) sample B; (c) sample C; (d) sample D.

(V_{acc}) of 5, 10, and 30 kV, with the emission current (I_e) of 10 μA. TEM characterization studies were carried out in a JEOL FX-2000 TEM (LaB6), as well as a FEI TecnaiF20 (FEG), both instruments operating at 200 kV. The beam currents in the FESEM, corresponding to each of the accelerating voltages at an emission current of 10 μA as measured by a Faraday cage were 0.015 μA, 0.021 μA, and 0.085 μA for acceleration voltage of 5 kV, 10 kV and 30 kV, respectively.[7] As shown in Fig. 2 the pore shrank from submicron dimensions to a few nanometers in the FESEM. The shrinkage rate decreased from $\sim$15.7 nm/min (average) to $\sim$6 nm/min (average), with a V_{acc} reduction from 30 kV to 10 kV. The pore did not shrink at all at 5 kV. These results imply that the shrinkage rate was correlated to the energy of the electron beam in the FESEM, and that there was a threshold between 5 and 10 kV; below this threshold, the shrinking phenomenon did not occur. Additionally, our observed rates were higher than those achieved by electron irradiation in the TEM.[3,6] Shrinkage rates of accelerating voltage and beam current versus shrinking rate are shown in Fig. 2(b).

Figures 3(a)–3(e) show the results of sample B (the oxide free membrane). Pore shrinkage was also observed in this sample during *in situ* FESEM imaging, and the shrinkage rate, which was $\sim$41 nm/min as shown in Fig. 3, was much higher than that for sample A. It is important to note that after the rapid shrinking, the silicon structure seemed to be damaged and reverted back towards the original shape. This

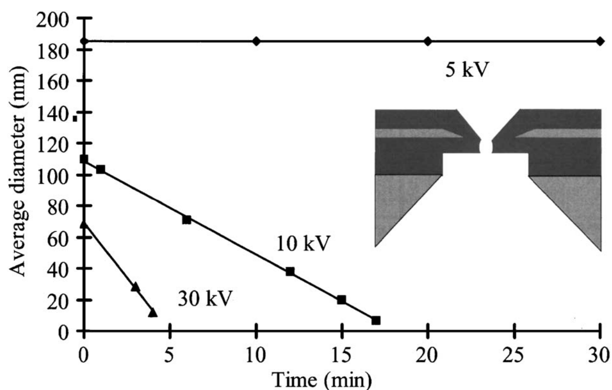

FIG. 2. Plot of pore diameter vs time for various accelerating voltages for sample A. Note: Average diameter=sqrt (long axis × short axis). The shrinkage rates for 10 and 30 kV were $\sim$6nm/min and 16nm/min, respectively.

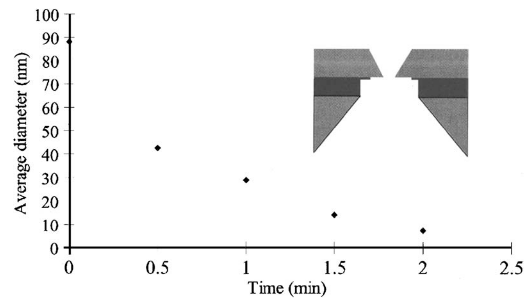

FIG. 3. Pore diameter vs time for sample B.

phenomenon needs further investigation. Samples C (pore in SOI layer/BOX not removed), and sample D (pore in SOI layer/no overhanging oxide) did not change at all in the FESEM. Thus, the pore shrinkage phenomenon appears to be related to both the material and structure of the pore. When the pore was in the silicon, with or without uniformly grown SiO_2, in a free standing membrane (samples A and B), it shrank. However, the pores made of pure oxide (the overhang in sample C), and the pore located on top of the BOX and handle silicon (sample D) did not change in the FESEM. In the case of samples C and D, the SOI layer is clearly constrained by the support BOX layer and could not move freely.

To help understand the metamorphosis of our nanopores, higher energy electron beam processing (TEM-based) was also carried out on the same type of samples and compared with the results from the FESEM. Sample A either shrank or expanded as reported previously by Storm *et al.* and followed the same rules derived by considering minimization of surface energy.[3] Figure 4(a) is a plot of the shrinkage rate versus electron dose rate (beam intensity) for the higher energy TEM based processing for sample A. We observed that

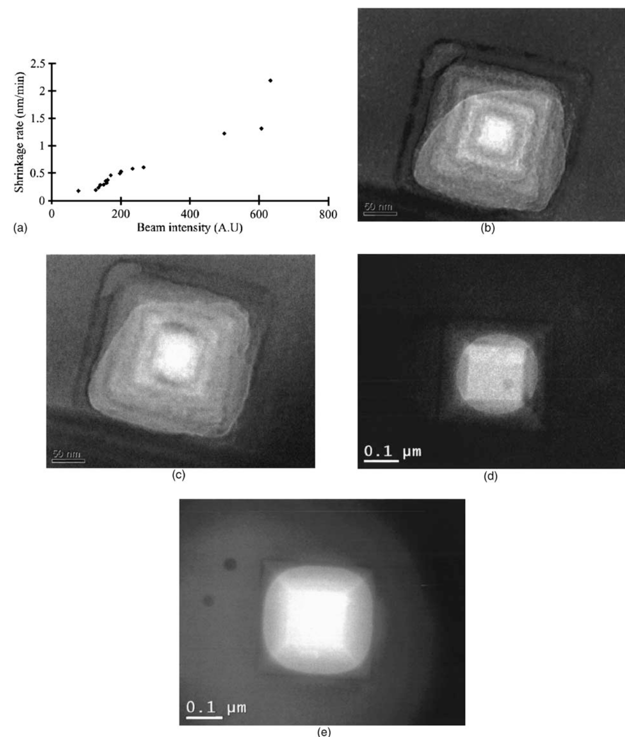

FIG. 4. TEM results of our experiments. (a) Plot of shrinking rate vs beam intensity for sample A. (b) and (c) Sample B did not have significant change in TEM. (d) and (e) Top oxide in sample C expanded in TEM.

Downloaded 27 Mar 2006 to 128.211.249.94. Redistribution subject to AIP license or copyright, see http://apl.aip.org/apl/copyright.jsp

a threshold in electron dose rate, at constant voltage, was needed to shrink pores. Figures 4(b) and 4(c) are the TEM images of sample B, and Figs. 4(d) and 4(e) are from sample C. As shown in sample B, the pore in a pure silicon layer exhibited insignificant change in the TEM. In sample C, the pore in the overhang oxide expanded, due to the fact that the diameter of the pore is greater than the oxide thickness.[3,6] Only the samples with an oxide shrank or expanded in the TEM, but those in pure silicon remained unchanged. This behavior was opposite to that observed in the FESEM. Moreover, only pore shrinkage occurred in the FESEM, while pores could either expand or shrink in the TEM, as shown in the case of sample C.

An obvious concern in these experiments is the possibility of hydrocarbon contamination being involved in the pore shrinkage process. We investigated this extensively and found no evidence linking this to the observed behavior. After creating the pores in the FESEM, we observed the pore diameter using both conventional bright field imaging in the TEM (JEOL 200 FX), and qualitative elemental mapping in a dedicated analytical TEM (FEI TecnaiF20). We found that the pore size was the same both before and after cleaning the samples in an argon-oxygen plasma (Fischione Model 1020 Plasma Cleaner), and energy filtered TEM imaging and electron energy loss spectroscopy showed no detectable carbon around the pore holes following the plasma cleaning procedure. Additionally, cleaning the samples prior to insertion into the FESEM with either Piranha solution (50:50 sulfuric acid:hydrogen peroxide) or argon-oxygen plasma cleaning did not alter the observed pore shrinkage behavior, nor did *ex post facto* cleaning with either the Piranha solution or the plasma process alter the pore sizes. In total, these observations strongly indicate the pore shrinkage process is not associated with hydrocarbon contamination.

It has been reported that irradiation by electron beams,[8–11] lasers,[12,13] and UV lights[14] causes damage in porous silicon and polycrystalline silicon. High-energy radiation disrupts the Si/Si and Si/H bonds (radiolysis) and results in dehydrogenation and the formation of surface defects. In our case, the SOI layer was heavily doped via ion implantation, and thus already had internal point defects and impurities remaining in the crystal structure from this procedure. When a silicon pore is observed in the FESEM, the high-energy electrons can transfer energy to the Si and SiO_2 layers; this can disrupt the bonding and potentially cause the silicon and oxygen atoms to diffuse towards the edge of the pore. Interestingly, whenever samples of the "A" type geometry were observed at 30 kV in the FESEM before the final thermal oxidation, the pore always expanded during observation in the TEM, independent of the ratio of pore diameter and oxide thickness. This implies that while the silicon was being imaged at 30 kV in the FESEM, the material is being affected by the electron irradiation.The maximum energy transfer by electrons to a silicon atom as a function of accelerating voltage has been reported earler.[15] Knock-on or displacement damage will only occur when the energy transfer exceeds the crystalline lattice displacement energy, which for silicon is ~15 eV. This corresponds to electron energy of more than ~150 keV. Since our operating conditions do not produce sufficient energy in the FESEM, it leads us to hypothesize that radiolysis and not knock-on damage is likely the mechanism leading to modification of the pore in the FESEM. The pore was not in its usual state thereafter, and thus the suggested mechanism of pore shrinking during electron irradiation in the TEM by Storm *et al.* could no longer be applied. It has been shown that deposited oxide on polycrystalline silicon gates can absorb 5.4 keV electron beam.[8] This could also shed some light on our observation that the shrinking rate of sample B was much higher than that for sample A. Direct irradiation generated more radiolysis induced defects in the silicon layers without scattering through the oxide layer. However, the mechanism needs further investigation.

We have presented a new technique to adjust the sizes of single nanopores in silicon and oxidized silicon layers and have proposed a possible mechanism explaining this phenomenon. Additionally, the shrinkage rate obtained using electron irradiation in the FESEM was found to be higher than in the TEM. This technique achieved good control over the pore size toward the deep nanoscale, yielding the ability to create pores of any size required by a specific application. Mass production of pores may be thus realized by combining a feedback system of beam current and automated control of the electron gun.

The authors acknowledge the support of the NASA Institute for Nanoelectronics and Computing (INAC) at Purdue under Award No. NCC 2-1363 for funding and supporting Hung Chang and Samir Iqbal, and by the U.S. DOE under Contract No. BES-MS W-31-109-Eng-38 for the work performed at ANL. The authors also want to acknowledge Ed Bagsell at Penn State University for electron beam lithography through the NSF-funded National Nanotechnology Infrastructure Network (NNIN). Partial wafer fabrication was performed at the University of Illinois at Chicago and at the Argonne National Labs (Dr. Derrick Mancini). The authors would like to express gratitude to Sara White and Bill Roth in Hitachi High Technologies America Inc. for valuable discussions.

[1]J. J. Kasianowicz, E. Brandin, D. Branton, and D. W. Deamer, Proc. Natl. Acad. Sci. U.S.A. **93**, 13770 (1996).
[2]J. Li, D. Stein, C. McMullan, D. Branton, M. J. Aziz, and J. A. Golovchenko, Nature (London) **412**, 166 (2001).
[3]A. J. Storm, J. H. Chen, X. S. Ling, H. W. Zandbergen, and C. Dekker, Nat. Mater. **2**, 537 (2003).
[4]J. Li, M. Gershow, D. Stein, E. Brandin, and J. Golovchenko, Nat. Mater. **2**, 611 (2003).
[5]H. Chang, F. Kosari, G. Andreadakis, M. A. Alam, G. Vasmatzis, and R. Bashir, Nano Lett. **4**, 1551 (2004).
[6]H. Chang, F. Kosari, G. Andreadakis, G. Vasmatzis, E. Basgall, A. H. King, and R. Bashir, in Proceedings of Hilton Head MEMS Conference, Hilton Head, South Carolina (2004), p. 204.
[7]Courtesy of Hitachi High Technologies America Inc. The numbers were determined by Faraday cup measurements. The model measured was S-5500, in which the beam current was identicle to the S-4800 used in our work.
[8]R. Nandakumar, P. Bhattacharya, and G. Kousik, Jpn. J. Appl. Phys., Part 1 **31**, 2651 (1992).
[9]J. L. Maurice, A. Riviere, A. Alapini, and C. Levy-Clement, Appl. Phys. Lett. **66**, 1665 (1995).
[10]M. Enachescu, E. Hartmann, and F. Koch, J. Appl. Phys. **79**, 2948 (1996).
[11]S. Borini, G. Amato, M. Rocchia, L. Boarino, and A. Mario Rossi, J. Appl. Phys. **93**, 4439 (2003).
[12]J. C. Barbour, D. Dimos, T. R. Guilinger, M. J. Kelly, and S. S. Tsao, Appl. Phys. Lett. **59**, 2088 (1991).
[13]J. Sarathy, S. Shih, K. Jung, C. Tsai, K. H. Li, D. L. Kwong, and J. C. Campbell, Appl. Phys. Lett. **60**, 1532 (1992).
[14]R. T. Collins, M. A. Tischler, and J. H. Stathis, Appl. Phys. Lett. **61**, 1649 (1992).
[15]C. R. Bradley and N. J. Zaluzec, Ultramicroscopy **28**, 226 (1989).

Downloaded 27 Mar 2006 to 128.211.249.94. Redistribution subject to AIP license or copyright, see http://apl.aip.org/apl/copyright.jsp